Enhancement of polar Kerr rotation in Fe/Al_2O_3 multilayers and composite systems

A. Bourzami, O. Lenoble,* and Ch. Féry
Laboratoire de Physique des Matériaux–UMR CNRS 7556, Université Henri Poincaré Nancy 1, Boîte Postale 239, 54506 Vandœvre-lès-Nancy Cedex, France

J. F. Bobo
LPMC–UMR CNRS 5830, INSA, Département Génie Physique, 31077 Toulouse Cedex 4, France

M. Piecuch
Laboratoire de Physique des Matériaux–UMR CNRS 7556, Université Henri Poincaré Nancy 1, Boîte Postale 239, 54506 Vandœvre-lès-Nancy Cedex, France

(Received 5 June 1998; revised manuscript received 4 November 1998)

We present theoretical and experimental results on the magneto-optic polar Kerr effect relative to several composite systems based on simple iron layers associated with amorphous alumina. The systems studied are either multilayers with a variable number of periods or trilayers. We have investigated the effect of the number of periods and of the individual layer thicknesses in the case of multilayers. Concerning trilayers, the role of the thickness of individual layers and of the stacking sequence is shown. We demonstrate that we can obtain very large values of Kerr rotation by optimization of the samples. A Kerr rotation close to 20° is, for instance, obtained with a very simple trilayer system: alumina/iron/alumina/Si substrate. [S0163-1829(99)01617-3]

I. INTRODUCTION

The magneto-optical Kerr effect could be considered as a very old phenomenon; however, it has been intensively studied in the past few years.[1–4] These studies are motivated, either by the potential utilization of this effect for high density recording systems or by the sensitivity of the Kerr effect for the detection of surface magnetism. In the case of multilayers, relatively few studies have tackled the problem and we only have a few theoretical published results.[3,4] The formalism used is based on the matrix method and calculates the wave propagation of light in a multilayer medium. To consider all the samples, we need to introduce two 4×4 matrices for each film, the first one relative to the interface and the second one relative to the propagation.

In this work, we use such a formalism to compute the Kerr effect (principally the rotation) produced by composite systems which are the stacking of a metallic magnetic material (iron) and a dielectric one (amorphous alumina). In that case, it is well known that we can have constructive interferences in the dielectric layer embedded between two metallic mirrors leading to Fabry-Perot-like cavity. This paper is a contribution to the study of the enhancement of the Kerr effect by collective additions of waves. We demonstrate here that one can construct devices with a very large Kerr effect, these important rotations being very easy to detect and useful for applications. We have tried to realize those samples which present high Kerr rotations by rf sputtering on Si(100) substrates.

The paper is divided into three parts. In Sec. II, we show theoretically that such huge Kerr rotations are predicted by the matrix formalism for definite thicknesses of the dielectric layer and for simple configurations of the device. In Sec. III, we describe the preparation of the layers and the Kerr effect measurement setup we have used. Finally, in Sec. IV, we present our experimental results and discuss them.

II. METHODOLOGY

In this formalism, the magnetic medium in which the electromagnetic waves propagate is considered to be homogenous and continuous with a dielectric permitivity tensor $\bar{\bar{\varepsilon}}_r$ given by Eq. (1):

$$\bar{\bar{\varepsilon}}_r=\tilde{n}_0^2\begin{pmatrix}1 & icQ & -ibQ\\ -icQ & 1 & iaQ\\ ibQ & -iaQ & 1\end{pmatrix}, \tag{1}$$

where $\bar{\bar{\varepsilon}}_r$ is given, to the first order in the magneto-optic parameter $Q=Q_1-iQ_2$, for a magnetization $\mathbf{M}$ following an arbitrary direction $\mathbf{u}(a,b,c)\cdot\tilde{n}_0=n_0-ik$ is the refractive index of the medium without magnetization. The relative permeability is taken equal to unity. The solution of the generalized Helmoltz equation gives two waves $\mathbf{E}^{(1,2)}$, which propagate in forward directions and two others $\mathbf{E}^{(3,4)}$, which propagate in the backward direction.[5] In a magnetic film, $\mathbf{E}^{(1,2)}$ can be interpreted like incident waves and $\mathbf{E}^{(3,4)}$ like reflected ones. In order to determine magneto-optic Kerr signals for a multilayer, we have to calculate the reflection matrix $[R]$ which relates the total reflected field $\mathbf{E}^r(E_s^r,E_p^r)$, to the incident one $\mathbf{E}^i(E_s^i,E_p^i)$. $[R]$ is determined by expressing the continuity of the tangential components of the total electromagnetic field ($\mathbf{E}$,$\mathbf{H}$) at the first interface (the subscripts s and p refer to the perpendicular and the parallel components to the incidence plane).

One of the methods used to compute the matrix $[R]$ is based on the establishment of two matrices.[4] In a Cartesian

coordinates system (xyz), where (yz) represents the incident plane and (xy) is coincident with the first interface, these two matrices are as follows.

A. The projection matrix [A] defined by [A]·E=F

[A] projects the total electric field $\mathbf{E}(E_s^i, E_p^i, E_s^r, E_p^r)$ in a film in a vector $\mathbf{F}(E_x, E_y, H_x, H_y)$ whose components at one interface are those of the corresponding total electromagnetic field ($\mathbf{E}$,$\mathbf{H}$). In order to determine [A], we first need to express the components of the magnetic field $\mathbf{H}^{(j)}$ of each wave as a function of the electric-field ones $\mathbf{E}^{(j)}$ by using Faraday's law:

$$\mathbf{H}^{(j)} = n^{(j)} \cdot \mathbf{w}^{(j)} \times \mathbf{E}^{(j)} \quad \text{with} \quad j = 1,2,3,4.$$

$\mathbf{n}^{(j)}$ are the corresponding refractive indices for the four waves $\mathbf{E}^{(1,2)}$ and $\mathbf{E}^{(3,4)}$:

$$n^{(1,2)} = \tilde{n}_0 \left(1 \pm \frac{Q}{2} \mathbf{u} \cdot \mathbf{w}_i \right) \quad \text{and} \quad n^{(3,4)} = \tilde{n}_0 \left(1 \pm \frac{Q}{2} \mathbf{u} \cdot \mathbf{w}_r \right).$$

$\mathbf{w}_i(0, w_y, w_z)$ and $\mathbf{w}_r(0, w_y, -w_z)$ are, respectively, the unit vectors of the incident and reflected wave directions.

The components of $E^{(j)}(E_x^{(j)}, E_y^{(j)}, E_z^{(j)})$ are not independent.[6] Therefore, $E_y^{(j)}$, $E_z^{(j)}$ must be expressed as a function of $E_x^{(j)}$. Finally, we have to express the components $E_x^{(1,2)}$ in the complex plane (E_s^i, iE_p^i), and $E_x^{(3,4)}$ in the complex plane (E_s^r, iE_p^r). This will lead to

$$[A] = \begin{bmatrix} 1 & 0 & 1 & 0 \\ \frac{i}{2} w_y^2 \left[\frac{\gamma_i}{w_z} - 2 \frac{\sigma_i}{w_y} \right] Q & (w_z - i a w_y Q) & -\frac{i}{2} w_y^2 \left[\frac{\gamma_r}{w_z} + 2 \frac{\sigma_r}{w_y} \right] Q & -(w_z + i a w_y Q) \\ -\frac{i}{2} \gamma_i \tilde{n}_0 Q & -\tilde{n}_0 & \frac{i}{2} \gamma_r \tilde{n}_0 Q & -\tilde{n}_0 \\ \tilde{n}_0 w_z & -\frac{i}{2} \frac{\gamma_i}{w_z} \tilde{n}_0 Q & -\tilde{n}_0 w_z & \frac{i}{2} \frac{\gamma_r}{w_z} \tilde{n}_0 Q \end{bmatrix}$$

where

$$\gamma_{i,r} = w_y b \pm w_z c = \mathbf{w}_{i,r} \cdot \mathbf{u}, \quad \sigma_{i,r} = w_y c \mp w_z b = (\mathbf{w}_{i,r} \times \mathbf{u}) \cdot \hat{\mathbf{x}}.$$

The sign of Q depends on the arbitrary positive direction of the magnetization. It should be noted that [A] is similar to that given by Zak *et al.*[8] However, the $[A]_{21}$ and $[A]_{23}$ elements are different. Nevertheless, in the particular cases of polar ($a=b=0$, $c=1$) and longitudinal ($a=c=0$, $b=1$) configurations, [A] gives exactly the same results.[4,8]

B. The propagation matrix [D]

[D] relates the total electric field $\mathbf{E}(E_s^i, E_p^i, E_s^r, E_p^r)$ at the two interfaces of the same film and is given by

$$\mathbf{E}(0) = [D] \cdot \mathbf{E}(d)$$

or

$$[D] = \begin{bmatrix} C_i \cdot e^{i\phi} & S_i \cdot e^{i\phi} & 0 & 0 \\ -S_i \cdot e^{i\phi} & C_i \cdot e^{i\phi} & 0 & 0 \\ 0 & 0 & C_r \cdot e^{-i\phi} & -S_r \cdot e^{-i\phi} \\ 0 & 0 & S_r \cdot e^{-i\phi} & C_r \cdot e^{-i\phi} \end{bmatrix},$$

where

$$C_{i,r} = \cos(\Omega_{i,r}), \quad S_{i,r} = \sin(\Omega_{i,r})$$

and

$$\Omega_{i,r} = \tilde{n}_0 \pi \frac{\gamma_{i,r}}{w_z} \frac{d}{\lambda} Q, \quad \phi = \tilde{n}_0 2\pi w_z \frac{d}{\lambda}.$$

λ is the wavelength and d is the thickness of the film.

The boundary equations written at each interface of a m-film multilayer, by using the matrices [A] and [D], lead to a relation between the electric field $\mathbf{E}_I(0)$ in the initial medium (air) to that $\mathbf{E}_F(d)$ in the final medium (substrate) through the transfer matrix [T]:[7]

$$\mathbf{E}_I(0) = [A_I^{-1}] \left(\prod_m [A_m][D_m][A_m^{-1}] \right) [A_F] \mathbf{E}_F(d) = [T] \mathbf{E}_F(d).$$

The final medium is semi-infinite, no wave is reflected ($E_{Fs}^r = E_{Fp}^r = 0$). Furthermore, we can deduce that the reflection matrix [R] may be expressed as a product of (2×2) block matrices [$T11$] and [$T21$] of [T].

For an s-polarized incident light, one can deduce from Ref. 9 that the Kerr rotation θ_{ks} and ellipticity ε_{ks} can be expressed as a function of Fresnel factors following Eq. (2):

$$\theta_{Ks} = \frac{1}{2} \tan^{-1} \left(\frac{2\,\mathrm{Re}(r_{ps}/r_{ss})}{1 - |r_{ps}/r_{ps}|^2} \right)$$

and

$$\varepsilon_{Ks} = \frac{1}{2} \sin^{-1} \left(\frac{2\,\mathrm{Im}(r_{ps}/r_{ss})}{1 + |r_{ps}/r_{ps}|^2} \right). \tag{2}$$

If r_{ps} is sufficiently small, the two last formulas can be approximated to define a complex Kerr rotation:

$$\tilde{\theta}_{Ks}=\theta_{Ks}+i\varepsilon_{Ks}\approx\frac{r_{ps}}{r_{ss}}.$$

For a *p*-polarized incident light, the ratio r_{ps}/r_{ss} is replaced by r_{sp}/r_{pp}. This macroscopic approach presents the advantage of being applicable to magnetic or to nonmagnetic media (by setting $Q=0$ in the last case). However, only the first reflection order is taken into account for each film.

III. EXPERIMENTAL DETAILS

A. Preparation and structural characterization of the samples

Films were deposited onto microelectronics-grade (100)-oxidized Si substrates maintained at room temperature in an Alcatel SCM 650 automated sputtering apparatus. Typically 99.5% pure Fe and Al_2O_3 targets were mounted on 10 cm diameter rf magnetron cathodes. The base pressure was 7×10^{-7} mb and 99.999% purified argon was introduced into the chamber through a pressure-regulated valve up to an operating pressure equal to 3×10^{-3} mb. Topological characteristics of the films have been studied by small-angles x-ray scattering (SAXS) with a Philips high-resolution diffractometer at Co $K\alpha1$ line ($\lambda=1.788\,92$ Å). These experiments were performed in $\theta/2\theta$ specular mode. Diffractograms exhibit several Kiessig fringes whose position and intensity are characteristic of the x-ray optical index (i.e., the density of the films), their thickness and their roughness. We used the standard recursive model[10] for the SAXS diffractograms simulation. SAXS simulations give us information about the sharpness of the interfaces: $\sigma(\text{air}/Al_2O_3)=20$ Å, $\sigma(Al_2O_3/\text{Fe})=11$ Å, and $\sigma(Al_2O_3/\text{Si})=10$ Å.

B. Optical and magneto-optical constants

In order to calculate Kerr rotation and ellipticity, we first have to determine the optical and magneto-optical constants relative to all materials in the multilayer system.

We used a Perkin-Elmer spectrophotometer (λ: 2300–26000 Å), to collect the reflection spectrum with a normal incidence of a 3600-Å-thick alumina film deposited onto a Si substrate. The spectrum was fitted in the 550–8000 Å range. Optical constants of silicon are given in Ref. 12, yielding the following refractive index n_A and thickness t_A (note the agreement with the SAXS experiments for the film thickness);

$$n_A=1.63+\frac{0.26\times10^6}{\lambda^2(\text{Å})},$$

$$t_A=3580\pm50\ \text{Å}.$$

Iron optical constants n_0 and k were determined by the ellipsometry method[13] applied to our experimental setup. Indeed, if the polarizer axe makes a small angle α with the p direction, the complex rotation θ_a due to metallic reflection, is given by

$$\tilde{\theta}a=\theta a+i\varepsilon_a=\frac{E_s^r}{E_p^r}=\frac{r_{ss}}{r_{pp}},\quad \alpha=\alpha\frac{\rho_s}{\rho_p}e^{i(\varphi_s-\varphi_p)}=\alpha\cdot\rho e^{i\varphi},$$

where (ρ_s,φ_s) and (ρ_p,φ_p) denote, respectively, the magnitudes and the phases of the reflection Fresnel factors r_{ss} and r_{pp}.

Therefore, θ_a and ε_a are linear functions of α. Their slopes, calculated by using the least-squares method, give ρ and φ. θ_a and ε_a are measured for a given α, compensating them with the rotation of the quarter-wave plate, respectively, in the F and $2F$ modes (θ_K and ε_K remain constant if no magnetic field is applied). It was shown in Ref. 14 that n_0 is given by

$$\tilde{n}_0{}^2=\sin^2\theta\left[1+tg^2\theta\left(\frac{1+\rho e^{j\varphi}}{1-\rho e^{j\varphi}}\right)^2\right].$$

The direct measurements of the refractive index are affected by the surface oxide of the film. In order to reduce this effect, we have deposited 500 Å of iron on a 3-mm-thick float-glass substrate. The sample is illuminated by the laser source through the substrate, with an incidence equal to 70°. The measurements are carried out on the second reflected spot which is extracted by a slit. The complex refractive index obtained is $\tilde{n}_0=2.32-i3.13$.

For the same sample configuration, the measured Kerr rotation and ellipticity in the longitudinal configuration and with an *s*-polarized incident light, are $\theta_{Ks}=121\,m°$ and $\varepsilon_{Ks}=25\,m°$. This leads to $Q=0.0284-i0.0038$.

The values obtained for $\tilde{n}_0$ and Q are close to those mentioned in Refs. 6, 7, and 8. Kerr ellipticity and rotation are measured by using the retardation modulation technique with an elasto-optic modulator.[10,11] The incidence angle is set to 10° in the polar configuration and to 70° in the longitudinal one. θ_k and ϕ_k are, respectively, obtained by the fundamental and the second harmonics detected by the lock-in amplifier tuned on the modulator frequency.

IV. RESULTS AND DISCUSSION

In a previous paper,[15] it has been shown that alumina/iron interfaces are smooth and have low interdiffusion in the case of multilayers, and that this system is thermodynamically stable up to 500 °C. Then, it was decided to study the magneto-optic properties of $[\text{Fe}(t_{\text{Fe}}\,\text{Å})/Al_2O_3(t_A\,\text{Å})]_m/\text{Si}$ multilayer systems. Kerr rotation appears at each magnetic interface. Thus, it seems clear that a Kerr rotation enhancement requires an important number of bilayers. Of course, a total iron thickness greater than the skin depth is useless. A few years ago, we tried this system with a set parameter: $m=20$ bilayers and for different iron and alumina thicknesses. We obtained a Kerr rotation as large as 2 degrees but the conclusion was deceptive without any correlation: a small change of the alumina or the iron thickness would lead to a dramatic decrease of the Kerr rotation. A better understanding of this system requires the use of the matrix formalism.

First, we have realized computer simulations which show that $Fe/Al_2O_3/Si$ bilayers give higher Kerr rotations than

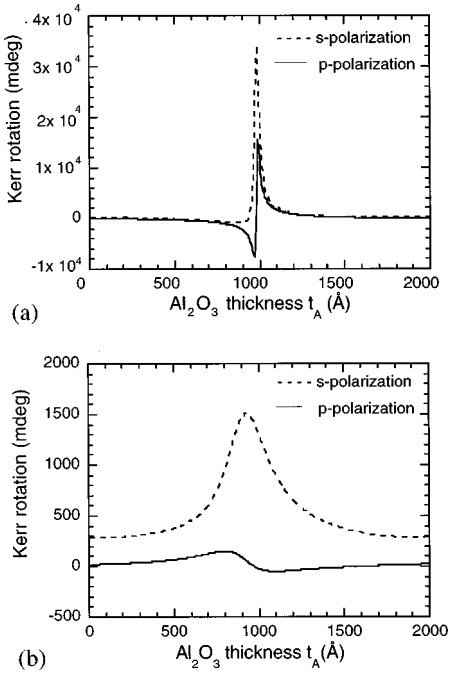

FIG. 1. Kerr rotation as a function of the alumina layer thickness (t_A) for Fe(20 Å)/Al_2O_3(t_A)/Si (a) and Al_2O_3(t_A)/Fe(20 Å)/Si systems (b).

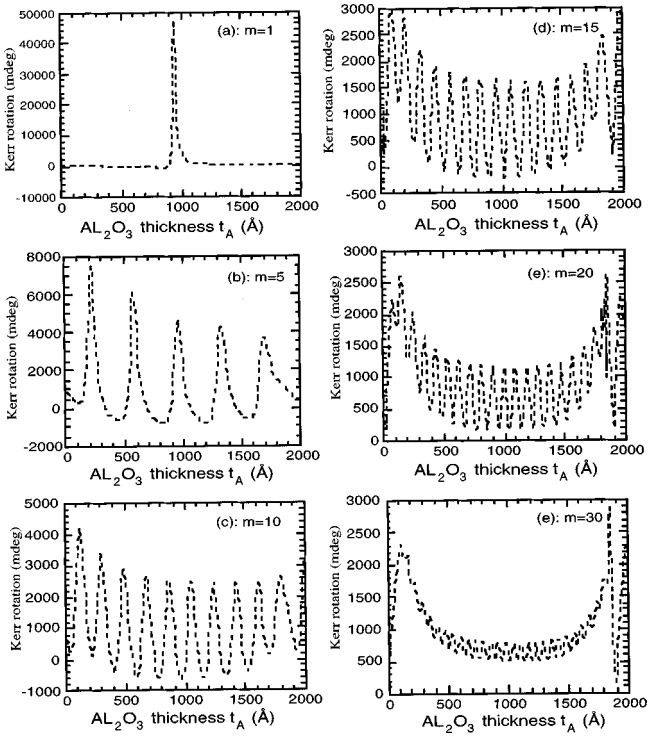

FIG. 2. Kerr rotation as a function of the alumina layer thickness (t_A) for a Al_2O_3(52 Å)/[Fe(20 Å)/Al_2O_3(t_A)]$_m$/Si system in *s* polarization (m=1,5,10,15,20,30).

Al_2O_3/Fe/Si ones (Fig. 1). This is explained by the fact that in the first case, the iron layer and the substrate can be considered like an optical cavity and then lead to an increase of the Kerr rotation essentially by reflection. The first optimum corresponds to constructive interference between the wave crossing the iron layer and reflected on the substrate and the wave reflected at the first alumina/iron interface. The second one corresponds to the constructive interference between the first wave and those reflected at the iron/alumina interface. This kind of amplifier is consistent with the fact that these samples, which give an important Kerr rotation, are relatively absorbent; the absorption coefficient is not determined, for instance.

Having studied the effect of stacking sequence, we know now that [Al_2O_3/Fe]$_m$/Si will give lower Kerr rotations than [Fe/Al_2O_3]$_m$/Si, but the top iron layer needs an alumina capping layer. Computer simulations give us information about its thickness which must be quite thinner. All samples were then protected by a 52 Å alumina layer. It remains now to optimize iron and alumina layer thicknesses (t_{Fe} and t_A) but also the number of bilayers (m) in Al_2O_3(52 Å)/[Fe(t_{Fe} Å)/Al_2O_3(t_A Å)]$_m$/Si systems.

In all cases, important Kerr rotations have been obtained with an amazing iron layer thickness which is as thin as 20 Å. Concerning the number of bilayers (m), Figs. 2(a)–2(f) represent calculated curves giving the ''*s*'' rotation, as a function of t_A in the case of multilayers for m equal to 1, 5, 10, 15, 20, and 30. Similar behavior is obtained in the case of ''*p*'' rotation. One can observe that all these curves exhibit oscillations with a large common period T which corresponds approximately to the double crossing made by the wave through the alumina, when reflected by the substrate. For θ=10° incidence (our case in polar configuration), this calculated period is equal to

$$T=\frac{\lambda}{2n_A\cos\theta_r}=1900\ \text{Å},$$

where θ_r is the refraction angle in alumina.

Therefore, the presented curves only concern thicknesses lower than 2000 Å. We must underline that, when the number of bilayers increases, m oscillations take place and correspond to the interferences relative to waves issued from all iron/alumina interfaces [Figs. 2(b)–2(f)]. One can observe that these curves look similar to those relative to luminous intensity diffracted by an optical grating. As for T, the period of these small oscillations corresponds to the optical thickness of the bilayer, divided by m. The last curves [6(e),6(f)] illustrate clearly that a small modification of t_A leads to an important evolution of the Kerr rotation. This result is very important because one would have thought that an increase of the number of bilayers would lead to a global Kerr rotation enhancement by a simple addition of rotation at each interface. Working with 20 bilayers few years ago, it is now obvious why we could not find any correlation.

Theoretically, we have shown the important parameters: let us look now at experimental results. We tried to reproduce the Kerr rotation peak in the case of Al_2O_3(52 Å)/[Fe(20 Å)/Al_2O_3(t_A Å)]$_m$/Si system with *s*- and *p*-polarized incident light. Samples have been realized by rf sputtering and results are presented in Figs. 3 and 4. Dependence of Kerr rotation in *s* as well as in *p* polarization, on the alumina layer thickness, is totally consistent with the predicted one and presents a peak close to T/2. Kerr rotation reaches strong values, up to 10° (Fig. 4), with an applied magnetic field equal to 7 kOe which does not allow the magnetic saturation

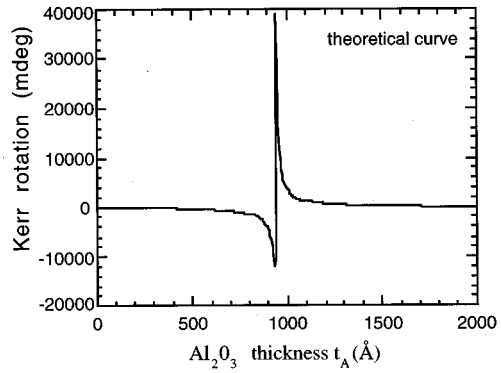

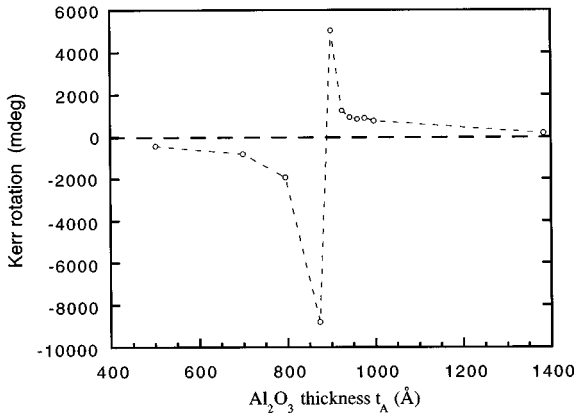

FIG. 3. Experimental Kerr rotation values: dependence with the alumina layer thickness (t_A) for a Al_2O_3(52 Å)/Fe(20 Å)/Al_2O_3(t_A)/Si system, in *p* polarization.

of the iron layers. Sample which presents the most important Kerr rotation was studied with another experimental setup[16] (able to saturate magnetically) and gives a θ_{Ks} equal to 20° (see Fig. 5).

One can notice that the optima positions correspond to an opposite phase ($T/2$) at which we must add 180° due to the reflection at alumina/substrate interface. In fact, to have an amplifier effect, this thickness must be slightly modified taking into account the retardation due to the cross through the first iron layer for the first optimum and of the retardation due to the reflection at the iron/alumina interface for the second optimum. We interpret the difference between theoretical and experimental results by the only taken account of reflections at the first order and more certainly by the approximate determination of the refractive indices. Moreover, in our calculations, we have considered perfect interfaces, while SAXS experiments indicate a roughness close to 10 Å.

As a discussion, we can say that our model is quite satisfactory and leads to a good agreement between experimental and theoretical results. From computer calculations, we have shown the possibility of obtaining an important Kerr rotation in polar configuration in *s* or *p* polarizations. The peak position is very sensitive to the refractive indices and it is quite difficult to determine with good accuracy.

Regarding the media storage, this system in polar configuration cannot be used because of the hysteresis loop which presents a small coercive field and of a hard perpendicular magnetic axis. Two ways may be considered: optimization of θ_k in systems with perpendicular magnetic anisotropy, and the same system but in a longitudinal configuration.

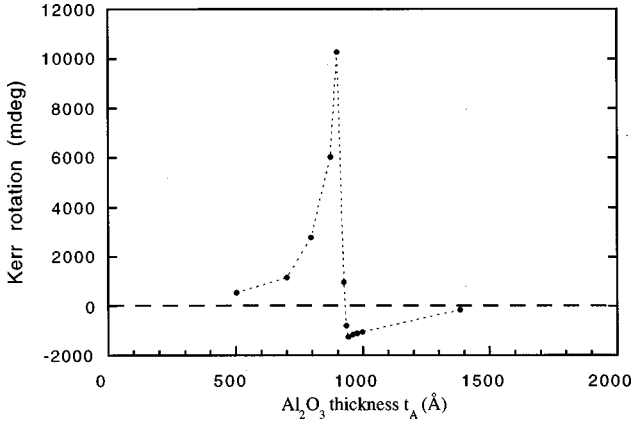

FIG. 4. Experimental Kerr rotation values: dependence with the alumina layer thickness (t_A) for a Al_2O_3(52 Å)/Fe(20 Å)/Al_2O_3(t_A)/Si system, in *s* polarization.

V. CONCLUSION

We have developed numerical simulations with the aim of determining Kerr ellipticity and rotation for an arbitrary magnetization direction, in *s*- and *p*-polarized light. We have then applied this formalism to the case of $(Al_2O_3/[Fe/Al_2O_3)]_m/Si$ multilayers and we have shown that it is possible to obtain important Kerr rotations with a more simple sample than the Al_2O_3/Fe/Al_2O_3/Si trilayer. Simulations had given the main way to obtain these important Kerr rotations: one must obtain a peak for an alumina layer thickness close to 1000 Å covered by an iron layer as thin as 20 Å and finally a protective alumina layer (52 Å).

The preparation of these samples by rf sputtering has allowed us to confirm the validity of our numerical simulations with measurements of Kerr rotations higher than 10° (with 7 kOe) and 20° (with saturated sample).

These systems are thermally stable and then lead to a good reproducibility of the results. For magneto-optical recording applications, it is important to look at systems in which the magnetization in the out-of-plane sample or in the longitudinal configuration.

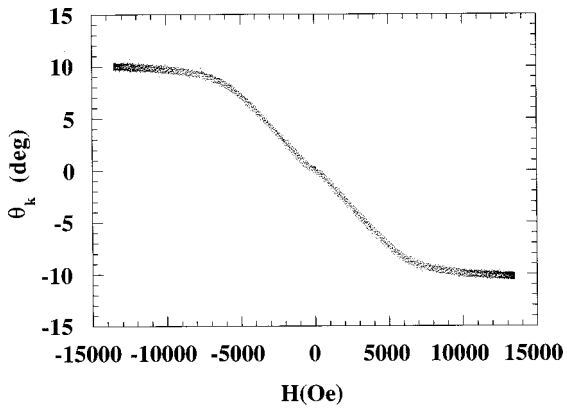

FIG. 5. Experimental Kerr rotation values: dependence with the alumina layer thickness (t_A) for a Al_2O_3(52 Å)/Fe(20 Å)/Al_2O_3(t_A)/Si system, in *s* polarization.

*Author to whom correspondence should be addressed.
[1] S. Visnovski, M. Nyvlt, V. Prosser, R. Lopusnik, R. Urban, J. Ferre, G. Penissard, D. Renard, and R. Krishnan, Phys. Rev. B **52**, 1090 (1995).
[2] H. R. Zhai, M. Lu, Y. Z. Miao, Y. B. Xu, S. M. Zhou, H. Wang, J. W. Cai, B. X. Gu, S. L. Zhang, and H. Y. Zhang, J. Magn. Magn. Mater. **115**, 20 (1992).
[3] T. Yoshino and S. Tanaka, Jpn. J. Appl. Phys. **5**, 989 (1966).
[4] J. Zak, E. R. Moog, C. Liu, and S. D. Bader, J. Magn. Magn. Mater. **89**, 107 (1990).
[5] S. Visnovski, Czech. J. Phys., Sect. B **36**, 625 (1986).
[6] G. Metzger, P. Pluvinage, and R. Torquet, Ann. Phys. (Paris) **10**, 5 (1965).
[7] J. Zak, E. R. Moog, C. Liu, and S. D. Bader, Phys. Rev. B **43**, 6423 (1994).
[8] J. Zak, E. R. Moog, C. Liu, and S. D. Bader, J. Magn. Magn. Mater. **88**, L261 (1990).
[9] C. C. Robinson, J. Opt. Soc. Am. **53**, 681 (1963).
[10] M. Piecuch and L. Nevot, Mater. Sci. Forum **59-60**, 93 (1990); K. Sato, J. Appl. Phys. **20**, 2403 (1981).
[11] K. Sato, *Magnetic Multilayers*, edited by L. H. Bennet and R. E. Watson (Academic, London, 1994), p. 277.
[12] J. Badoz, M. Billardon, J. C. Canit, and M. F. Russel, J. Opt. **8**, 373 (1977).
[13] E. D. Palik, *Handbook of Optical Constants of Solids* (Academic, London, 1985), p. 565.
[14] M. Born and E. Wolf, *Principles of Optics*, 6th ed. (Pergamon, London, 1991), p. 615.
[15] O. Lenoble, J. F. Bobo, L. Hennet, H. Fischer, Ph. Bauer, and M. Piecuch, Thin Solid Films **275**, 64 (1996).
[16] K. Postava, J. F. Bobo, M. D. Ortega, B. Raquet, H. Jaffres, E. Snoeck, and M. Goiran, J. Magn. Magn. Mater. **88**, 8 (1996).